ELSEVIER

Chemical Geology 234 (2006) 1 – 16

CHEMICAL GEOLOGY
INCLUDING
ISOTOPE GEOSCIENCE

www.elsevier.com/locate/chemgeo

Effect of chemical composition of water on the oxygen-18 and carbon-13 signature preserved in cryogenic carbonates, Arctic Canada: Implications in paleoclimatic studies

D. Lacelle [a,b,*], B. Lauriol [b], I.D. Clark [a]

[a] *Ottawa—Carleton Geoscience Centre, University of Ottawa, 140 Louis Pasteur, Ottawa, ON, Canada, K1N 6N5*
[b] *Department of Geography, University of Ottawa, 60 University St., Ottawa, ON, Canada, K1N 6N5*

Received 22 December 2005; received in revised form 24 March 2006; accepted 10 April 2006

Abstract

This study examines the $\delta^{18}O$ and $\delta^{13}C$ composition of cryogenic carbonate deposits in relation to the initial $\delta^{18}O$, $\delta^{13}C_{DIC}$ and chemical composition of the water from which it precipitated. This study focuses on cryogenic calcites precipitated in relation to aufeis aggradation since it offers the possibility of examining the chemical and isotopic partitioning that occurs during freezing. The studied aufeis are located in the western Canadian Arctic (YT and NWT), a region underlain mostly by limestone bedrock, and southern Baffin Island (NU), an area of crystalline bedrock. The results indicate that the $\delta^{18}O$ composition of cryogenic calcite from a carbonated environment are slightly depleted over that of the initial $\delta^{18}O$ of the parent water, while those from a non-carbonated environment are strongly depleted over the initial $\delta^{18}O$ of the parent water as a result of the lower calcite saturation state of the parent water. This suggest that the $\delta^{18}O$ of cryogenic carbonates not only depends on the initial $\delta^{18}O$ composition of the parent water and the temperature at which the carbonate precipitated, but also on the calcite saturation state of the parent water and kinetic inhibitions during calcite precipitation. Given that the aggradation of aufeis occurs under closed-system freezing, the residual water will become progressively depleted in $\delta^{18}O$ as a result of the removal of heavier isotopes in the ice. In addition, freezing imparts a concentration of solutes in the residual water, which leads to an increase in calcite saturation index. Therefore, carbonate precipitated in equilibrium from water that has a low calcite saturation index will have a highly depleted $\delta^{18}O$ composition over that of the initial $\delta^{18}O$ values of the parent water since the calcite saturation state will only be exceeded in the late stage of freezing. By contrast, solute and isotopic partitioning during freezing has little effect on the $\delta^{13}C$ of the cryogenic carbonates as it tends to reflect that of the initial $\delta^{13}C_{DIC}$ value of the parent water. These findings have significant implications in the use of cryogenic carbonates in paleoclimate studies. Care must be taken when interpreting the $\delta^{18}O$ signature preserved in cryogenic carbonates since their signature might be modified by freezing prior to their precipitation, which will lead to a lighter $\delta^{18}O$ composition of the cryogenic carbonates. Therefore, it would be difficult to use the $\delta^{18}O$ composition of cryogenic carbonates as a direct proxy in paleoclimatic reconstruction unless details about the chemical composition of parent waters are known. Nevertheless, the $\delta^{13}C$ composition of the cryogenic carbonates that precipitated under closed-system conditions can allow insights into the different water sources contributing to carbonate precipitation.

Keywords: Cryogenic carbonates; Aufeis; Stable isotopes of oxygen; Stable isotopes of carbon; Northern Yukon Territory; Southern Baffin Island; Canadian Arctic

* Corresponding author. Department of Earth Sciences, University of Ottawa, 140 Louis Pasteur, Ottawa, ON, Canada, K1N 6N5. Fax: +1 613 562 5192.
E-mail address: dlace056@uottawa.ca (D. Lacelle).

0009-2541/$ - see front matter © 2006 Elsevier B.V. All rights reserved.
doi:10.1016/j.chemgeo.2006.04.001

1. Introduction

Currently, with the exception of ice cores (Dansgaard, 1982; Fisher et al., 1998; Epica Community Members, 2004), freshwater endostromatolites (Clark et al., 2004) and Tertiary speleothems (Lauriol et al., 1997), direct climate proxies in polar regions are rare. As a consequence, cryogenic carbonate deposits, which form by CO_2 degassing during the freezing of water containing calcium and bicarbonate, have been receiving growing interest as paleoclimatic proxies due to the sensitivity of polar regions to the recent changes in climate. In polar regions, cryogenic carbonates have been reported from various environments, including in freezing caves (Clark and Lauriol, 1992; Zak et al., 2004), on the surface of aufeis along riverbeds (Hall, 1980; Pollard, 1983; Lauriol et al., 1991; Clark and Lauriol, 1997), in lakebeds of the Dry Valleys of Antarctica (Nakai et al., 1975), on the upper surface of clasts in deglaciated regions (Hallet, 1976; Hillaire-Marcel et al., 1979; Souchez and Lemmens, 1985; Sharp et al., 1990; Fairchild et al., 1993; Blake, 2005) and on the lower surface of clasts within the active layer (Swett, 1974; Bunting and Christensen, 1978; Forman and Miller, 1984; Marlin et al., 1993; Courty et al., 1994).

Generally, quantitative reconstructions of paleotemperatures rely on the analysis of the stable isotope ratio of oxygen ($^{18}O/^{16}O$) preserved in the carbonates and the global $\delta^{18}O$–T °C relation developed by Dansgaard (1964), providing that the waters from which the carbonate precipitated reflect the local mean annual air temperature. Carbon isotopes ($^{13}C/^{12}C$) are also included whenever they contribute significant paleoclimatic information. However, before cryogenic carbonates can be regarded as reliable archives of past climatic conditions, two key issues relating to the interpretation of the $^{18}O/^{16}O$ and $^{13}C/^{12}C$ ratios preserved in cryogenic carbonate must be addressed. The first is to verify if the $^{18}O/^{16}O$ ratio preserved in cryogenic carbonate deposits reflects that of the local mean annual air temperature, since freezing is a fractionating process that imparts a progressive depletion on the initial $^{18}O/^{16}O$ ratio of the parent water. The second issue is related to the effect of freezing on the $^{13}C/^{12}C$ ratio in cryogenic carbonate. According to Clark and Lauriol (1992), Socki et al. (2001) and Zak et al. (2004), the $^{13}C/^{12}C$ ratio in cryogenic carbonate is dependent on the rate of reaction at which the carbonate precipitates, which can lead to severe kinetic fractionation of ^{13}C between the cryogenic carbonate and the escaping CO_2. If the cryogenic carbonate precipitated from waters that were modified by such secondary processes, their $^{18}O/^{16}O$ and $^{13}C/^{12}C$ ratio might not be useful in quantitative paleoclimatic studies.

In this study, the chemical and isotopic ($^{18}O/^{16}O$; $^{13}C/^{12}C$) partitioning that is occurring between the water feeding aufeis in distinct geological settings (carbonated vs. non-carbonated) and their associated mineral precipitates are examined to evaluate the potential of the cryogenic aufeis carbonate as direct paleoclimatic proxies. The studied aufeis are located in the western Canadian Arctic, a region dominantly underlain by limestone bedrock, and southern Baffin Island (NU), an area of crystalline bedrock (Fig. 1). The objective of this study will be reached by *i*) determining the chemical composition and stable isotope ratios of O, H and C of the waters feeding the aufeis; *ii*) determining the stable isotope ratios of O and H of the ice-layers composing the aufeis; and *iii*) determining the stable isotope ratios of O and C of the cryogenic aufeis calcite deposits associated with aufeis growth. This should provide insights into the concurrent segregation of solutes and stable isotope partitioning that occurs during freezing between water and the precipitating carbonate in areas of limestone and granitic bedrock. This study will also evaluate whether cryogenic aufeis carbonates precipitate in isotopic equilibrium with the parent water, or if kinetic conditions control their formation.

2. Background on aufeis and their associated mineral precipitates

Aufeis (icings) are sheet-like masses of layered ice that accumulate on river channels by the freezing of successive overflows of perennial groundwater-fed springs upon exposure to cold air (Van Everdingen, 1974; Tolsikhin and Tolsikhin, 1976). Most aufeis are located in permafrosted limestone environments (Akerman, 1982; Van Everdingen and Allen, 1983; Pollard, 1983; Van Everndingen, 1988; Lauriol et al., 1991; Clark and Lauriol, 1997; Pollard, 2005) as they offer the greatest possibility to host perennial groundwater discharge through the development of open fractures and fissures, which facilitate the circulation of groundwater through taliks (Clark and Lauriol, 1997; Clark et al., 2001). As a result, the groundwaters feeding aufeis are typically characterized by a $Ca–HCO_3$ facies. The geochemical signature of the groundwaters feeding the aufeis is important since the process of aufeis aggradation is associated with the production of mineral precipitates within the ice-layers by solute expulsion during freezing (Hall, 1980; Pollard, 1983; Clark and Lauriol, 1997). The most common mineral precipitated during aufeis growth are calcite ($CaCO_3$), gypsum

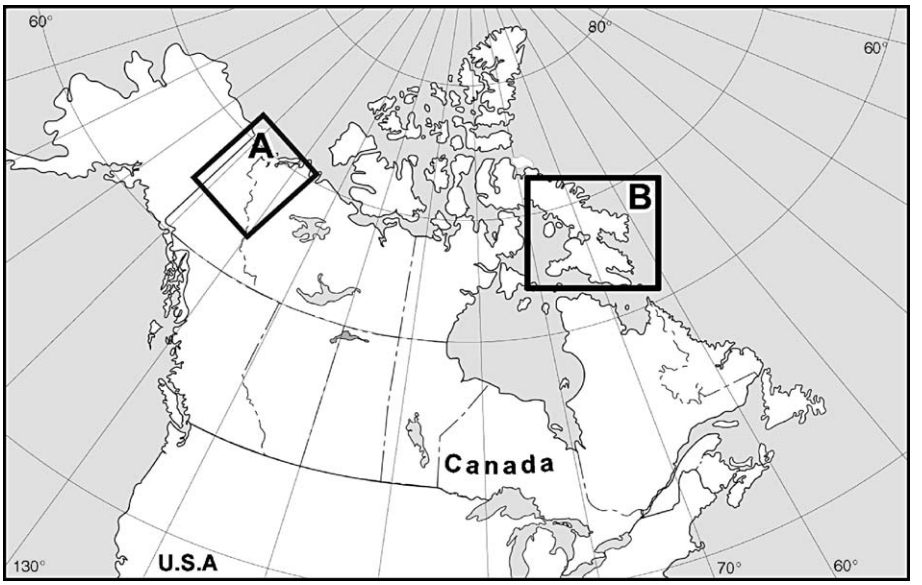

Fig. 1. Location of the regions studied in the Canadian Arctic. The boxes A and B identify the areas mapped in Figs. 2 and 4 respectively.

($CaSO_4 \cdot 2H_2O$), halite (NaCl) and ikaite ($CaCO_3 \cdot 6H_2O$) (Hall, 1980; Clark and Lauriol, 1997; Pollard, 2005). The mineral precipitates are released from the aufeis onto its surface and surroundings during the thaw season. Residual accumulations of calcite powders of up to 18,000 m^3 were reported by Hall (1980) on the surface of aufeis located along the north slopes of Alaska.

3. Site descriptions

3.1. Carbonated environment: western Canadian Arctic (YT and NWT)

Numerous aufeis can be found along the beds of rivers in the western Canadian Arctic, and three were examined in this study: the Babbage River, Fish Hole Creek and Little Fish Creek aufeis (Fig. 2). The Babbage River and Fish Hole Creek aufeis (68°48′N; 138°47′W) are located at the southern footslope of the Barn's Range in the British Mountains, an area underlain by Jurassic–Lower Cretaceous marine shale and siltstone of the Kingak Formation (Norris, 1977). Little Fish Creek aufeis (67°45′N; 136°19′W) is located in the White Mountains near McDougall Pass. The White Mountains are part of the Richardson Mountains and consist of a circular limestone and dolomite massif from the Carboniferous Lisburne group flanked by highly folded and faulted Mesozoic shales and sandstones (Norris, 1975). These aufeis cover an approximate surface area of a few km^2 or less, which is far less than the Firth River aufeis (31.5 km^2), the largest aufeis located in the British Mountains, northern Yukon Territory (Clark and Lauriol, 1997).

The studied aufeis in the western Canadian Arctic are associated with fault zones in carbonated bedrock. The Babbage River and Fish Hole Creek aufeis are located downstream from a regional strike that intersects the riverbeds on which the aufeis are located. Little Fish Creek aufeis is also located in a region with geological structures (Fig. 3). An orthogonal fault crosses an anticlinal structure formed by Permian and Jurassic sediments in an SW–NE direction, perpendicular to the Fish Creek valley. Consequently, the presence of faults and strikes probably enhances groundwater discharge from the carbonate terrain, which promotes the growth of aufeis.

The climate in the western Canadian Arctic is part of the polar continental regime. The climate recorded at Shingle Point, located along the coastline of the Beaufort Sea, reports a mean annual air temperature of −10 °C (January T °C −25 °C; July T °C 11 °C; Environment Canada, 2004), while the mean annual air temperature at Fort McPherson, located 100 km east of the Richardson Mountains, is −8.8 °C (January T °C −30 °C; July T °C 15 °C; Environment Canada, 2004). Precipitation in the western Canadian Arctic is generally light. The total annual precipitation along the coastline averages between 125 to 185 mm yr^{-1} but increases to 366 mm yr^{-1} at Fort McPherson due to orographic effects (Environment Canada, 2004). Vegetation in the western Canadian Arctic is largely arctic tundra with forest–tundra ecotone along the valleys, grading into

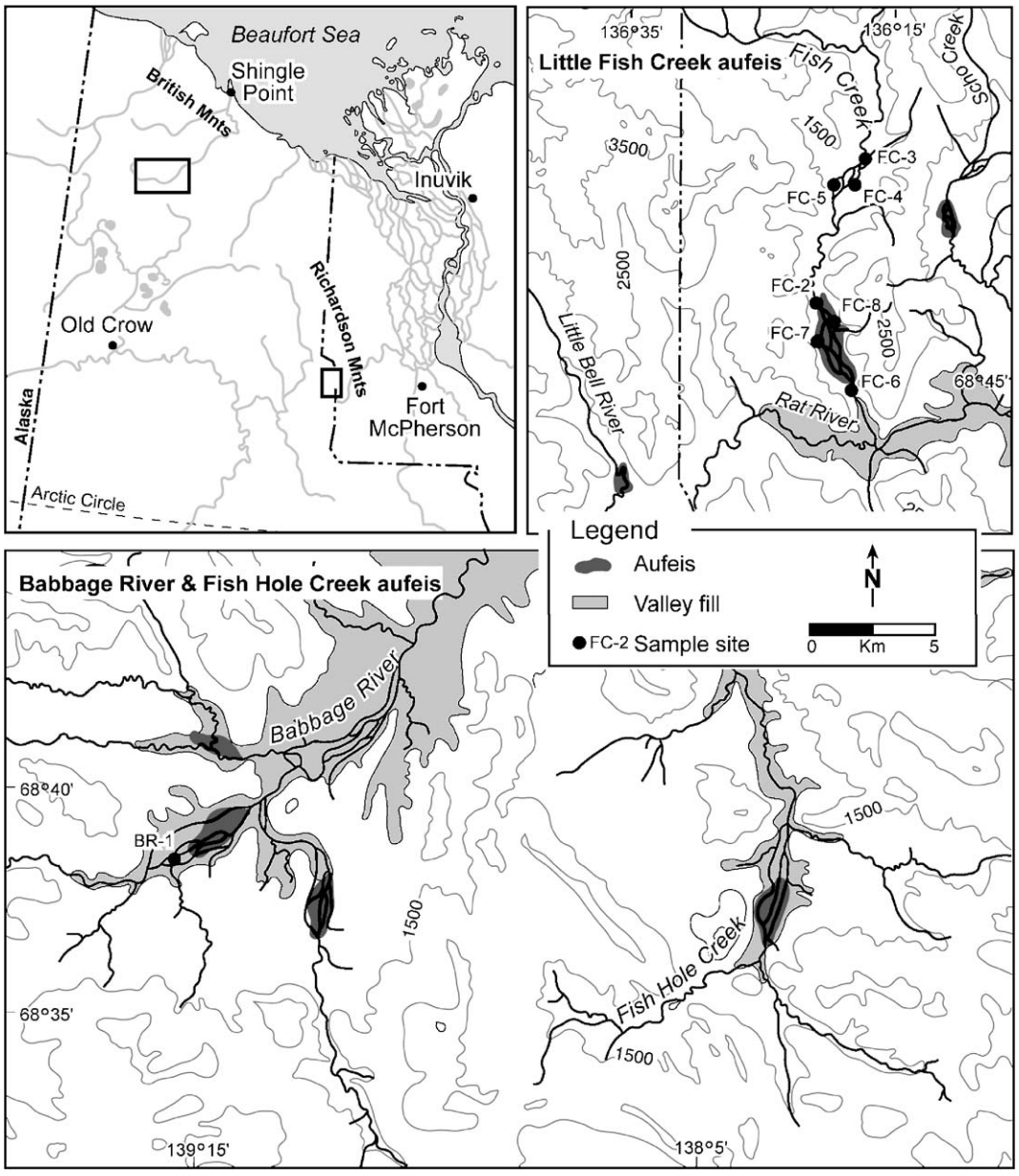

Fig. 2. Maps showing the location of the Babbage River, Fish Hole Creek and Little Fish Creek aufeis sampled in the western Canadian Arctic along with the water sample sites.

alpine tundra with increasing elevation. Barren limestone outcrop dominates at higher elevations.

3.2. Non-carbonated environment: southern Baffin Island (NU)

Aufeis in a non-carbonated environment are rare, but a few were found in Akshayuk Pass (66°44′N; 65°00′W), a 98 km long U-shaped glacial valley incised into the Penny highlands on southern Cumberland Peninsula, Baffin Island, NU (Fig. 4). The most impressive and largest aufeis in Akshayuk Pass is Highway Glacier aufeis, which accumulates near the terminus of Highway Glacier, a tributary glacier of the 6000 km^2 Penny Ice Cap (Fig. 4). An examination of historical aerial photographs (1948) and field observations (2004) revealed that Highway Glacier aufeis underwent a geographical shift that is likely related to the receding Highway Glacier (Fig. 4). It is suggested that the aufeis is fed by subglacial meltwaters circulating through a

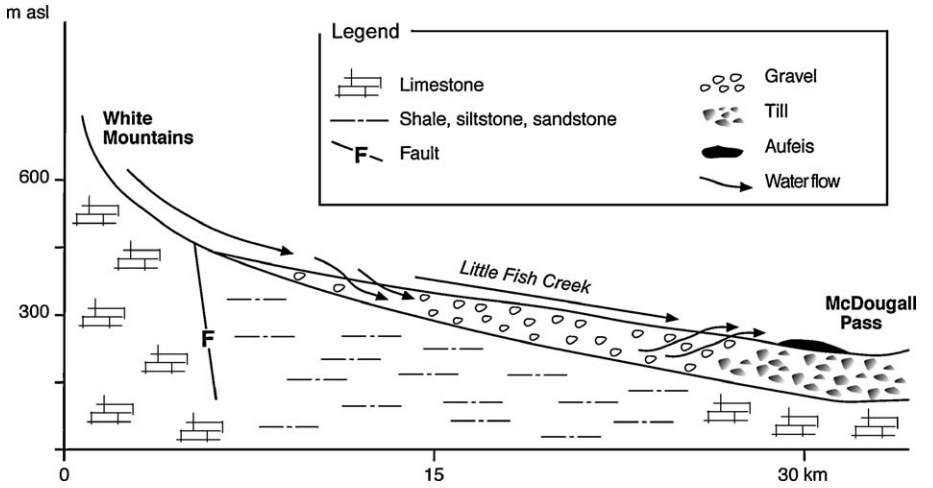

Fig. 3. Schematic diagram of a cross-section from the White Mountains to McDougall Pass showing recharge and circulation of groundwater feeding the Little Fish Creek aufeis (NWT).

proglacial talik, and the presence of permafrost in the proglacial zone forces the groundwater to the surface. In early summer 2004, Highway Glacier aufeis measured 1 km long, up to 400 m wide and 3–4 m thick, giving it an approximate surface area of 0.5 km^2. Other aufeis in Akshayuk Pass are located at the foothill of Turnweather Glacier and along the Weasel River near Thor shelter. These aufeis cover a surface area of less than 0.5 km^2.

Bedrock in Akshayuk Pass consists primarily of granitic rocks of the Precambrian Canadian Shield, medium to coarse-grained gneiss and quartz monzonites (Dyke et al., 1982). Carbonate bedrock is absent from the area, but fracture-filling calcite provides a carbon source that can assist in the precipitation of cryogenic carbonates.

The climate in Akshayuk Pass is part of the polar maritime regime and is highly variable due to the presence of the Penny Ice Cap in the highlands. The climate recorded at the nearest meteorological station, the hamlet of Pangnirtung, reports a mean annual air temperature of −10.4 °C (January T °C −28 °C; July T °C 7 °C) and total annual precipitation of nearly 400 mm (Environment Canada, 2004). Vegetation in Akshayuk Pass ranges from very patchy and open on the slopes, to lush tundra meadows near the flood plain. Arctic shrubs such as dwarf birch, willow, heather, and blueberry form a continuous carpet in sheltered valleys, while tussocks of grasses and sedges grow in less favourable areas.

4. Methodologies

4.1. Sampling technique

The Babbage River, Fish Hole Creek and Little Fish Creek aufeis, located in the western Canadian Arctic, were sampled in July 1996 and 1997. Highway Glacier aufeis, located in southern Baffin Island, was sampled in July 2004. At all sites, water samples for cations analysis were field filtered (0.45 μm pore diameter) and collected in 20 ml pre-rinsed polyethylene bottles, with subsequent acidification using ultra-pure nitric acid. Filtered, unacidified samples were collected for anion analysis in 20 ml pre-rinsed polyethylene bottles. Water samples for the measurement of the stable isotope ratios of oxygen ($^{18}O/^{16}O$) and hydrogen (D/H) were collected unfiltered in 20 ml polyethylene bottles. Filtered water samples were collected unpreserved in 40 ml glass amber bottles for the determination of dissolved inorganic carbon (DIC) and its stable isotope ratio ($^{13}C/^{12}C$). In addition, individual ice-layers of the aufeis were collected using a ice axe. The ice was melted in the field and then poured unfiltered in polyethylene bottles for the analysis of the stable isotope ratios of oxygen and hydrogen. Mineral precipitates found on the surface of the aufeis were collected in sterile roll-top bags.

4.2. Analytical procedures

Field measurements included temperature and pH of the water. Alkalinity was measured in the field during our visits to the western Canadian Arctic aufeis only, and in the laboratory for the southern Baffin Island water samples.

Major cations were analyzed by Inductively Coupled Plasma Atomic Emission Spectroscopy. The anions were analyzed using a Dionex DX-100 ion chromatograph. All samples were run in duplicate and the analytical reproducibility was ±5% for the cations and ±10% for the anions.

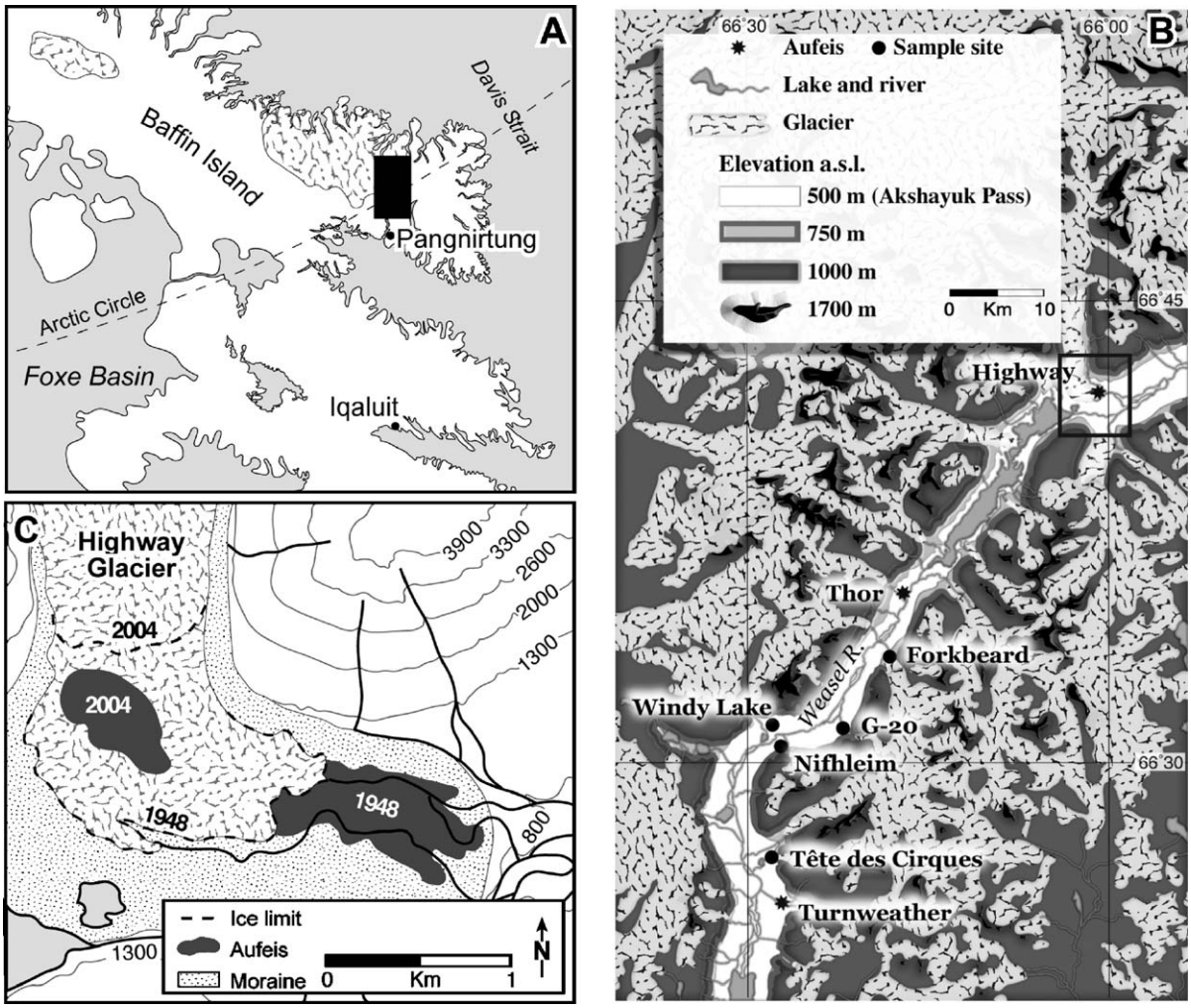

Fig. 4. A) Map showing the location of Akshayuk Pass, a 98 km long glacial valley on southern Cumberland Peninsula, Nunavut. B) Map showing the location of Highway Glacier aufeis in Akshayuk Pass along with the water sample sites. C) Map showing the geographical shifting of Highway Glacier aufeis between 1948 (aerial photograph T214-L59) and 2004 (field observations).

The $^{18}O/^{16}O$ ratio of the water samples was determined on CO_2 isotopically equilibrated with the water at 25 °C (analytical reproducibility of ±0.1‰). The D/H ratio was measured on H_2 isotopically equilibrated with the water at 25 °C using a Pt based catalyst (analytical reproducibility of ±1.5‰). Both stable isotope measurements were made on the same sample using a Gas Bench II interfaced with a Finnigan Mat Delta$^+$ XP isotope mass spectrometer at the G.G. Hatch Laboratory (University of Ottawa). Results are presented using the δ-notation, where δ represents the parts per thousand difference of $^{18}O/^{16}O$ or D/H in a sample with respect to Vienna Standard Mean Ocean Water (VSMOW).

The $^{13}C/^{12}C$ ratio of the dissolved inorganic carbon (DIC) in the water samples from the northern Yukon Territory was determined upon return from the field by acidification under vacuum and cryogenic purification of the CO_2, which was then analyzed on a VG SIRA-12 mass spectrometer. The DIC concentrations and $^{13}C/^{12}C$ of the DIC in the water samples from southern Cumberland Peninsula were determined on a TIC-TOC analyser model OI-1010 interfaced to a Finnigan Mat Delta$^+$ isotope ratio mass spectrometer at the G.G. Hatch Laboratory following the wet oxidation technique described by St-Jean (2003). The DIC concentrations were normalized using internal standards and the analytical precision is ±0.002 ppm. The $^{13}C/^{12}C$ ratios of the DIC are expressed in δ-notation, where δ represents the parts per thousand difference of $^{13}C/^{12}C$ in a sample with respect to the Vienna Pee-Dee Belemnite (VPDB) standard. Analytical precision is ±0.2‰.

The $^{18}O/^{16}O$ and $^{13}C/^{12}C$ ratios of the calcite deposits were determined on CO_2 gas produced by reacting the powdered calcite with 100% phosphoric acid (H_3PO_4) in glass septum vials for 24 h at 25 °C. The evolved CO_2 gas was analyzed in continuous flow using a Gas Bench II interfaced to a Finnigan Mat Delta$^+$ XP isotope mass spectrometer at the G.G. Hatch Laboratory. Stable isotope data for C and O are expressed in δ-notation, where δ represents the parts per thousand difference of $^{18}O/^{16}O$ and $^{13}C/^{12}C$ in a sample with respect to the Vienna Pee-Dee Belemnite standard (VPDB). Analytical reproducibility is ±0.15‰ for both isotopes.

4.3. Data analysis

The temperature, pH and geochemical composition of the waters were entered into PHREEQC, an hydrogeochemical program (Parkhurst and Appelo, 1999), to calculate the partial pressure of CO_2 (log pCO_2) and saturation state of the water with respect to calcite (SIcal). The partial pressure of CO_2 is determined from pH and HCO_3^- measurements from the following equation:

$$\log\ pCO_2 = -pH + \log([aHCO_3^-]/K_{CO2}K_1) \quad (1)$$

where $aHCO_3^-$ is the ion activity, K_{CO2} is the equilibrium constant for CO_2 and K_1 is the first dissociation constant of H_2CO_3. This equation assumes that HCO_3^- is the main contributor to alkalinity, which is the case given the pH range of the surface and spring waters.

In PHREEQC, the saturation state of the water with respect to calcite is calculated by the following equation:

$$SIcal = \log aCa^{2+} + \log aCO_3^{2-} - KCaCO_3 \quad (2)$$

where SIcal is the saturation index of calcite, aCa^{2+} and aCO_3^{2-} are the respective ion activities and $KCaCO_3$ is the equilibrium solubility product for calcite. The solution is undersaturated if SIcal is <0, at equilibrium if SIcal=0, or supersaturated if SIcal>0.

5. Results

5.1. Water chemistry

Based on the ternary diagram of the geochemical composition of the waters sampled in the western Canadian Arctic and in Akshayuk Pass, three principal geochemical facies are identified. The geochemical facies can be distinguished according to the local bedrock lithology and groundwater recharge circulation pathways (Fig. 5).

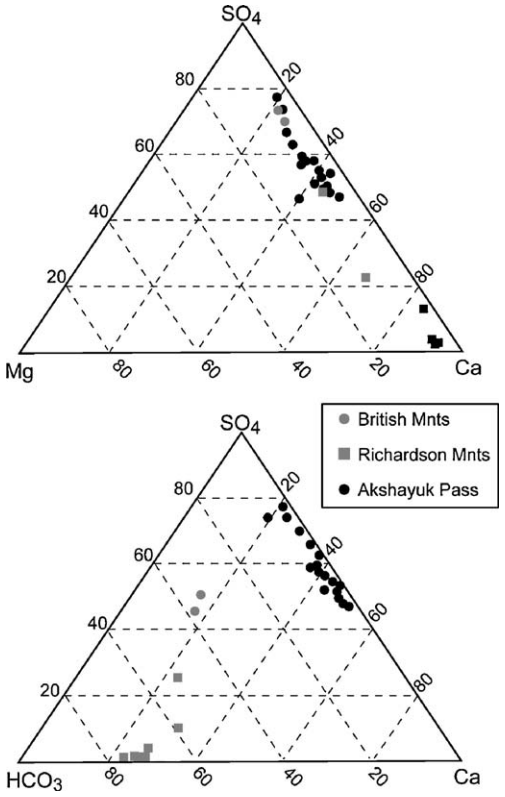

Fig. 5. Ternary diagrams of the geochemical composition of the waters feeding the Babbage River and Fish Hole Creek (British Mountains), Little Fish Creek (Richardson Mountains) and Highway Glacier aufeis (Akshayuk Pass).

The first group is associated with the surface and spring waters feeding the Babbage River and Fish Hole Creek aufeis, which are located in the British Mountains. These waters are highly mineralized (specific conductivity in the 1372 to 3723 µS/cm range), are characterized by a Ca–HCO_3–SO_4 facies and have pH values around 8 (Table 1). For comparison, the waters feeding the Firth River aufeis (Clark and Lauriol, 1997) have a similar geochemical composition (Table 1). This suggests that the Ca–HCO_3–SO_4 facies might be characteristic of groundwater circulating through the limestone bedrock of the Lisburne Group, which is the dominant lithological group in the British Mountains. The calcite saturation indices of the surface and spring waters circulating in this region are also close to saturation due to carbonate dissolution. The surface waters in the area have $\delta^{18}O$ values averaging −22.4±0.7‰.

The second group is associated with waters feeding the Little Fish Creek aufeis, located in an area underlain

Table 1
Geochemical (mg/L) and isotopic (‰) data from surface waters and springs in the northern Yukon Territory and Northwest Territories

Sample ID	T °C	pH	Ca	Mg	Na	K	Cl	ALK	SO_4	SIcal	log pCO_2	$\delta^{18}O$	$\delta^{13}C_{DIC}$
British Mountains													
Surface waters — Babbage River													
BR-1	4.0	8.4	43.8	10.8	198.0	7.0	185.9	98.8	148.3	0.2	−3.5	*n.d.*	*n.d.*
Firth River[a]													
Average	*4.3*	*7.7*	*48.4*	*3.1*	*0.3*	*0.2*	*n.d.*	*151.0*	*10.0*	*−0.3*	*−2.6*	*−22.4*	*−7.2*
STDEV	*1.5*	*0.2*	*15.1*	*0.9*	*0.1*	*0.1*	*n.d.*	*26.0*	*6.0*	*0.4*	*0.2*	*0.7*	*1.4*
Springs — Firth River[a]													
Average	*2.4*	*7.6*	*62.8*	*5.3*	*0.2*	*0.3*	*0.8*	*153.4*	*55.5*	*−0.2*	*−2.5*	*n.d.*	*−5.6*
STDEV	*1.7*	*0.2*	*28.1*	*2.7*	*0.1*	*0.3*	*0.2*	*29.3*	*72.9*	*0.3*	*0.2*	*n.d.*	*1.8*
Richardson Mountains													
Surface waters — Little Fish Creek													
FC-2	5.4	7.0	34.0	1.9	0.3	0.3	0.3	100.0	1.2	−1.1	−2.0	−22.0	−7.8
FC-3	1.2	5.0	5.7	0.9	0.3	0.1	0.4	11.0	1.9	−4.8	−4.1	−21.5	−0.8
FC-4	3.5	6.5	30.6	0.9	0.3	0.1	0.6	79.0	4.6	−1.8	−3.1	−21.8	−0.9
FC-5	1.8	4.9	6.6	1.0	0.3	0.3	0.1	15.0	7.4	−4.8	−3.4	−20.8	−0.1
FC−6	2.3	7.4	46.0	2.6	0.4	0.8	0.6	119.0	1.2	−0.6	−2.5	−21.6	−0.2
FC-7	0.6	7.6	44.1	2.4	0.4	1.4	0.4	145.0	0.9	−0.3	−2.6	−20.8	−0.2
FC-8	0.4	7.3	43.2	2.1	0.3	0.7	0.4	124.0	1.0	−0.8	−2.3	−21.1	−10.6
Average	*2.2*	*6.5*	*30.0*	*1.7*	*0.3*	*0.5*	*0.4*	*84.7*	*2.6*	*−2.0*	*−2.9*	*−21.4*	*−2.9*
STDEV	*1.8*	*1.1*	*17.2*	*0.7*	*0.1*	*0.5*	*0.2*	*53.1*	*2.5*	*1.9*	*0.7*	*0.5*	*4.4*
Springs — Little Fish Creek													
	1.5	8.6	72.3	13.3	4.7	0.6	2.1	160.7	96.6	0.8	−3.5	*n.d.*	*n.d.*

n.d.: no data.
[a] Data from Clark and Lauriol (1997).

by Carboniferous limestone and Mesozoic shale and sandstone in the Richardson Mountains. The surface waters feeding Little Fish Creek aufeis have a low mineralization (specific conductivity=410 μS/cm), a Ca–HCO_3 facies and pH values in the 4.9 to 7.6 range (Table 1). The waters feeding Little Fish Creek aufeis probably circulated through the highly faulted Mesozoic shale and sandstone overlying the marine limestone, as indicated by the lower pH values and salinity compared to those feeding the Babbage River and Fish Hole Creek aufeis located in the British Mountains. The calcite saturation indices of the waters feeding the Little Fish Creek aufeis, which averages −2.0±1.9, is further supportive of a shallow groundwater circulating through the Mesozoic shale and sandstone. The surface waters feeding Little Fish Creek aufeis have invariant $\delta^{18}O$ values (−21.4±0.5‰; n=7).

The third group is associated with waters feeding Highway Glacier aufeis, located in an area underlain by granitic, gneiss and quartz monzonite bedrock in southern Cumberland Peninsula, Baffin Island. The glacial meltwaters have a very low solute concentration (<7 mg/L), are characterized by a Ca–Mg–SO_4 facies and a pH in the 5.4 to 6.6 range (Table 2). The glacial meltwaters are also highly undersaturated with respect to calcite mineral (SIcal<−5) due to the local bedrock lithology. The glacial meltwaters have $\delta^{18}O$ values averaging −22.5±1.8‰ (n=31), which reflects that of the average $\delta^{18}O$ of precipitation in the area (Fisher et al., 1998).

Carbon isotope measurement of the dissolved inorganic carbon ($\delta^{13}C_{DIC}$) of surface waters feeding Little Fish Creek and Highway Glacier aufeis are shown in Tables 1 and 2. The surface waters feeding the Little Fish Creek aufeis have $\delta^{13}C_{DIC}$ values in the −10.6‰ to −0.1‰ range. The glacial meltwaters in Akshayuk Pass have similar $\delta^{13}C_{DIC}$ values, ranging from −11.3‰ to −3.1‰. The $\delta^{13}C_{DIC}$ values surface and spring waters feeding the Firth River aufeis are also similar as they range between −8.9‰ and −3.3‰ (Clark and Lauriol, 1997). This range in $\delta^{13}C_{DIC}$ values is attributed to varying degree of exchange with atmospheric CO_2 during surface flow.

The $\delta^{18}O$ and δD compositions of the individual ice-layers from the Babbage River, Fish Hole Creek, Little Fish Creek and Highway Glacier aufeis are illustrated in Fig. 6. Since an isotopic mass-balance must be preserved during freezing, the $\delta^{18}O$ values of the individual ice-layers represent the average $\delta^{18}O$ composition of the waters feeding the aufeis. The $\delta^{18}O$ composition of the studied aufeis ranges between −23.5‰ and −19.4‰ and show no significant differences among the different geological regions (limestone and granitic). They are also

Table 2
Geochemical (mg/L) and isotopic (‰) data from glacial meltwaters in Akshayuk Pass, southern Cumberland Peninsula (NU)

Sample ID	T °C	pH	Ca	Mg	Na	K	ALK	SO_4	SIcal	log pCO_2	$\delta^{18}O$	$\delta^{13}C_{DIC}$
Akshayuk Pass												
HG-03-04	*n.d.*	*n.d.*	4.45	0.40	1.13	0.59	*n.d.*	*n.d.*	*n.d.*	*n.d.*	−21.6	*n.d.*
HG-04-04	*n.d.*	*n.d.*	3.12	b.d.	0.21	b.d.	*n.d.*	*n.d.*	*n.d.*	*n.d.*	−21.0	*n.d.*
HG-05-04	*n.d.*	*n.d.*	2.94	0.32	0.48	0.59	*n.d.*	*n.d.*	*n.d.*	*n.d.*	−22.7	*n.d.*
HG-06-04	*n.d.*	*n.d.*	2.95	0.33	0.44	0.56	*n.d.*	*n.d.*	*n.d.*	*n.d.*	−22.7	*n.d.*
HG-08-04	*n.d.*	*n.d.*	1.03	0.12	1.63	0.76	*n.d.*	*n.d.*	*n.d.*	*n.d.*	−21.0	*n.d.*
HG-10-04	*n.d.*	*n.d.*	1.22	0.12	0.25	b.d.	*n.d.*	*n.d.*	*n.d.*	*n.d.*	−22.2	*n.d.*
HG-11-04	*n.d.*	*n.d.*	2.11	0.10	2.68	1.62	*n.d.*	*n.d.*	*n.d.*	*n.d.*	−21.0	*n.d.*
HG-12-04	*n.d.*	*n.d.*	2.64	b.d.	1.57	0.69	*n.d.*	*n.d.*	*n.d.*	*n.d.*	−22.9	*n.d.*
HG-13-04	*n.d.*	*n.d.*	2.67	0.32	0.54	0.70	*n.d.*	*n.d.*	*n.d.*	*n.d.*	−22.8	*n.d.*
HG-14-04	*n.d.*	*n.d.*	0.83	b.d.	0.10	b.d.	*n.d.*	*n.d.*	*n.d.*	*n.d.*	−22.6	*n.d.*
HG-15-04	*n.d.*	*n.d.*	0.83	b.d.	2.51	1.18	*n.d.*	*n.d.*	*n.d.*	*n.d.*	−22.8	*n.d.*
HG-21-04	*n.d.*	*n.d.*	1.18	b.d.	0.17	b.d.	*n.d.*	*n.d.*	*n.d.*	*n.d.*	−22.4	*n.d.*
FG-101-03	7.8	5.7	0.22	0.04	b.d.	b.d.	0.02	0.73	−7.3	−4.4	−22.0	−9.6
FG-110-03	9.2	5.7	0.24	0.04	b.d.	b.d.	0.02	0.94	−7.3	−4.4	−22.0	−11.3
G20-61-03	4.3	6.5	1.72	0.22	b.d.	b.d.	0.11	2.42	−5.7	−4.5	−22.0	−4.1
G20-71-03	4.3	6.5	1.48	0.19	b.d.	b.d.	0.12	2.26	−5.7	−4.5	−21.9	−6.5
G20-81-03	4.1	6.1	1.38	0.18	b.d.	b.d.	0.06	1.76	−6.3	−4.4	−22.0	−6.6
NG-41-03	5.6	5.9	1.71	0.39	0.94	b.d.	0.04	3.55	−6.3	−4.4	−22.0	−6.7
NG-42-03	1.3	6	2.58	0.89	1.31	b.d.	0.04	3.07	−6.2	−4.5	−22.1	−5.3
NG-51-03	5.5	6.4	1.36	0.31	0.65	b.d.	0.09	2.19	−5.9	−4.5	−21.9	−4.2
NG-52-03	4.8	6.1	1.60	0.38	0.94	b.d.	0.07	4.00	−6.2	−4.4	−22.0	−5.9
SG-82-03	3.6	6.5	2.11	0.19	0.46	b.d.	0.10	2.08	−5.7	−4.6	−21.8	−4.5
SG-86-03	4.7	6.1	1.94	0.17	0.34	b.d.	0.06	1.87	−6.1	−4.4	−21.9	−4.5
SG-90-03	4.1	6.5	2.01	0.14	0.31	b.d.	0.10	2.54	−5.7	−4.6	−22.0	−6.3
SG-91-03	9.5	6.6	0.31	0.05	b.d.	b.d.	0.11	1.23	−6.3	−4.6	−22.0	−9.9
TCG-09-04	5.0	5.6	1.27	0.29	0.40	b.d.	0.14	b.d.	−6.4	−3.5	−22.7	−9.9
TCG-27-03	4.0	6.3	0.81	0.16	b.d.	b.d.	0.09	1.00	−6.3	−4.4	−22.5	−10.8
TCG-28-03	5.0	6.4	0.94	0.18	b.d.	b.d.	0.11	1.52	−6.0	−4.4	−22.5	−9.2
TCG-30-03	4.8	5.4	1.01	0.20	0.32	b.d.	0.02	1.73	−6.7	−4.2	−22.5	−8.6
WG-119-03	6.0	6.5	1.82	0.24	b.d.	b.d.	0.11	1.92	−5.7	−4.5	−22.0	−3.7
WG-125-03	8.6	6.4	1.90	0.26	0.33	b.d.	0.09	2.16	−5.8	−4.5	−22.0	−3.1
Average	*5.3*	*6.2*	*2.09*	*0.29*	*0.88*	*1.11*	*0.08*	*2.06*	*−6.2*	*−4.4*	*−22.5*	*−6.9*
STDEV	*1.9*	*0.3*	*2.54*	*0.28*	*0.94*	*1.07*	*0.04*	*0.80*	*0.5*	*0.2*	*1.8*	*2.6*

Sample code: HG=Highway Glacier; FG=Forkbeard Glacier; G20=G20 Glacier; NG=Nifhleim Glacier.
SG=Sivingavuk Glacier; TCG=Tête des Cirques Glacier; WG=Windy Lake Glacier.
n.d. : no data.
b.d. : below detection limit.

very similar to the $\delta^{18}O$ composition of surface and spring waters feeding the aufeis (Tables 1 and 2).

5.2. Mineral precipitates

Mineral precipitates in the form of loose powders were present on the surface of all studied aufeis. The mineralogy of the precipitates collected from the Babbage River, Fish Hole Creek and Little Fish Creek aufeis was determined by powdered X-ray diffraction and calcite was the only mineral present. By contrast, XRD analysis indicated that the mineral precipitates collected on the surface of Highway Glacier aufeis consisted of a mixture of calcite, quartz and gypsum. Strontium isotope measurements ($^{87}Sr/^{86}Sr$) suggest that the source of silicate in the mineral deposits collected at Highway Glacier aufeis is derived from the crystalline bedrock (Fig. 7). The local granitic bedrock has a radiogenic $^{87}Sr/^{86}Sr$ ratio (0.7885±0.0358; n=5) that is considerably higher than the fracture-filling calcites (0.7261 to 0.7409; n=2). The mineral precipitates have $^{87}Sr/^{86}Sr$ ratios averaging 0.7719±0.003 (n=2), similar to the $^{87}Sr/^{86}Sr$ ratio measured in the local bedrock. This suggests that the cryogenic calcite deposits on the surface of Highway Glacier aufeis incorporated an important fraction of silicate derived from the bedrock by glacial erosion, which released silt-sized particles in the glacial meltwaters, or that the calcium that assisted in their precipitation is derived from silicate weathering (e.g. Jacobson et al., 2002; Hossein et al., 2004).

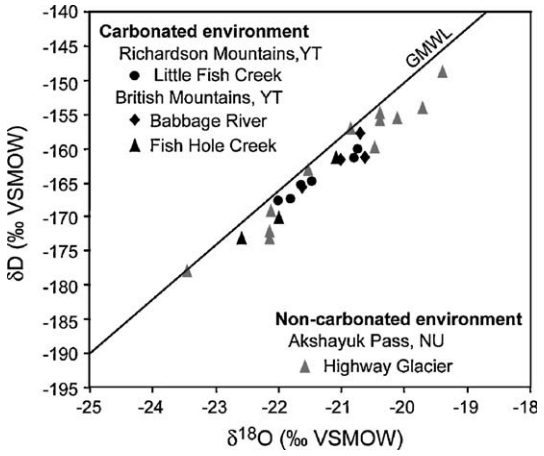

Fig. 6. $\delta^{18}O$ and δD composition of individual ice-layers from the Babbage River, Fish Hole Creek, Little Fish Creek and Highway Glacier aufeis. The global meteoric water line (GMWL) is shown for comparison purposes.

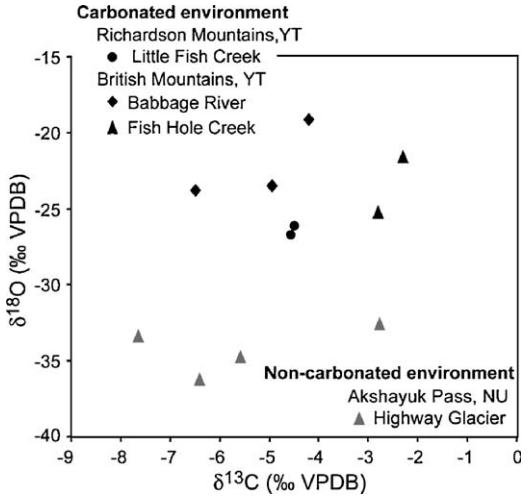

Fig. 8. $\delta^{18}O$ and $\delta^{13}C$ composition of cryogenic calcite collected from the surface of the Babbage River, Fish Hole Creek, Little Fish Creek and Highway Glacier aufeis.

The $\delta^{13}C$ and $\delta^{18}O$ composition of the cryogenic aufeis calcite deposits are presented in Fig. 8. The $\delta^{13}C$ values of cryogenic calcite collected from the Babbage River, Fish Hole Creek and Little Fish Creek aufeis average -5.1 ± 1.3‰, -2.6 ± 0.4‰ and -4.5 ± 0.1‰ respectively. Those from Highway Glacier aufeis are slightly more depleted, with $\delta^{13}C$ values between -7.6‰ and -2.8‰. The $\delta^{18}O$ values of cryogenic calcite from the Babbage River and Fish Hole Creek and Little Fish Creek aufeis average -22.2 ± 2.6‰, -23.5 ± 2.6‰ and -26.5 ± 0.2‰ respectively. By contrast, the calcite component of the mineral precipitates from Highway Glacier aufeis have some of the most depleted

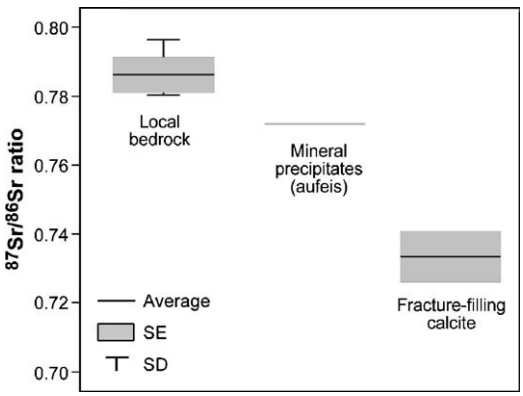

Fig. 7. Radiogenic strontium measurements of the mineral precipitates, local bedrock and fracture-filling calcite sampled in Akshayuk Pass. The $^{87}Sr/^{86}Sr$ ratios were determined by thermal ionization mass spectrometry (TIMS) on a Finnigan Mat Triton at Carleton University. Measured ratios were corrected for mass fractionation using $^{86}Sr/^{88}Sr=0.1194$.

$\delta^{18}O$ values reported in the literature for cryogenic aufeis calcite deposits, with $\delta^{18}O$ values ranging from -36.3‰ to -32.6‰.

6. Discussion

6.1. Oxygen-18 partitioning and chemical segregation during closed-system freezing

A comparison of the $\delta^{18}O$ composition of cryogenic aufeis calcite collected from carbonated and non-carbonated geological settings in the Canadian Arctic provides some insight into the chemical and isotopic partitioning that occurs during freezing. The $\delta^{18}O$ values of cryogenic aufeis calcite deposits from the Babbage River (-22.2 ± 2.6‰) and Fish Hole Creek (-23.5 ± 2.6‰) aufeis are much more enriched than those from Little Fish Creek aufeis (-26.5 ± 0.2‰) and Highway Glacier aufeis (-34.3 ± 1.6‰). Under most circumstances, the $\delta^{18}O$ of calcite is estimated from the $\delta^{18}O$ of the parent water and temperature at which calcite precipitated. Therefore, the $\delta^{18}O$ composition of the parent water from which the cryogenic aufeis calcite precipitated can be calculated by converting the $\delta^{18}O_{VPDB}$ values of the cryogenic calcite to the VSMOW scale using Coplen's equation:

$$\delta^{18}O_{VSMOW} = 1.03091\ \delta^{18}O_{VPDB} + 30.91‰ \quad (3)$$

(Coplen et al., 1983)

and using the fractionation factor for equilibrium exchange of ^{18}O between calcite and water ($\varepsilon^{18}O\ CaCO_3$–

H_2O at 0 °C = 34.4‰ VSMOW; Bottinga, 1968). For the Babbage River and Fish Hole Creek aufeis, this gives $\delta^{18}O$ values of −26.3 ± 2.6‰ and −27.7 ± 2.6‰ respectively for the parent water from which the cryogenic calcite precipitated (Fig. 9). However, the cryogenic calcite from Little Fish Creek and Highway Glacier aufeis precipitated from a parent water that had a much more depleted $\delta^{18}O$ composition, −30.8 ± 0.2‰ and −38.8 ± 1.6‰ respectively (Fig. 9). This is quite surprising given that the average $\delta^{18}O$ composition of the individual ice-layers composition the aufeis is much more enriched, with $\delta^{18}O$ values in the −23.5‰ to −19.4‰ range (Fig. 6).

Fig. 10 provides some interesting insights into the possible cause of this discrepancy, where a strong positive relation exists between the average $\delta^{18}O$ composition of the cryogenic aufeis calcite and the average calcite saturation state of the waters feeding the aufeis. This suggests that the $\delta^{18}O$ composition of the cryogenic calcite not only depends on the initial $\delta^{18}O$ composition of the parent water, but that it might also be influenced by the calcite saturation state of the parent water prior to freezing. Based on field observations (Heldmann et al., 2005) and $\delta^{18}O$ stratigraphy of aufeis ice (Clark and Lauriol, 1997), which shows a Rayleigh-type depletion trend within the individual ice layers, the aggradation of aufeis occurs under closed-system conditions. Under such conditions, the freezing of water imparts a progressive depletion in $\delta^{18}O$ in the residual water due to the preferential incorporation of the heavier isotopes in the ice. It should be noted that this progressive ^{18}O depletion trend in the residual water

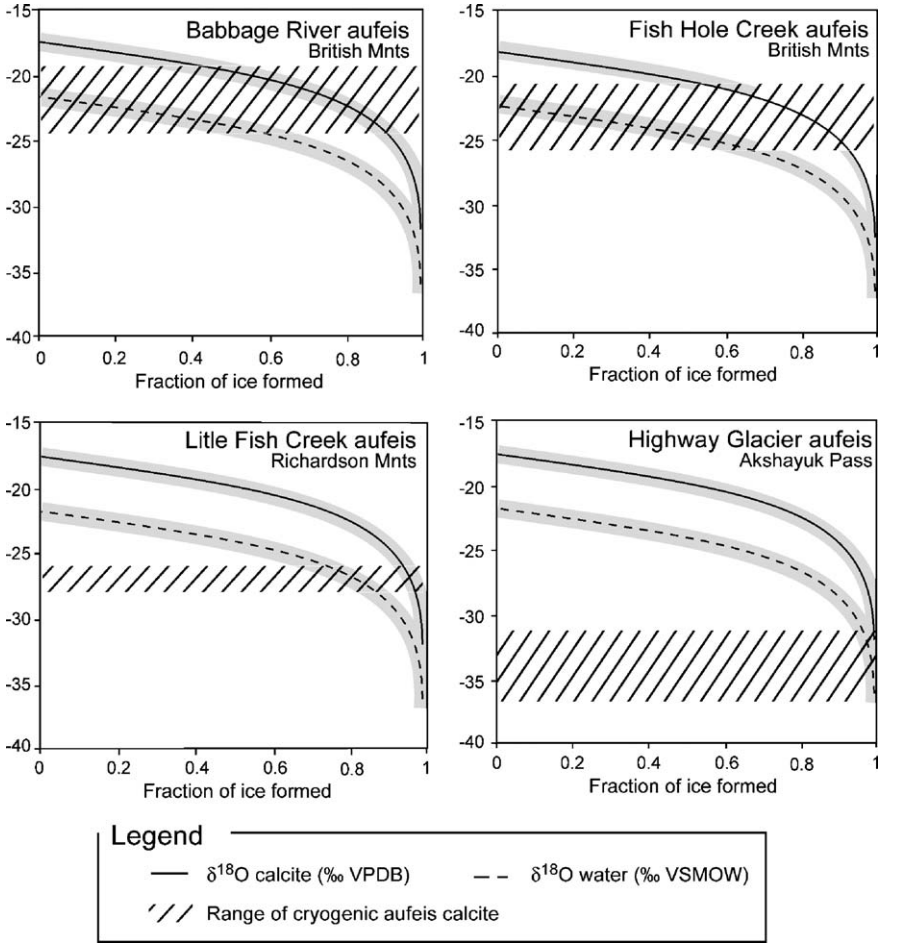

Fig. 9. Numerical modeling of the $\delta^{18}O$ evolution of water during closed-system freezing using a Rayleigh-type fractionation. The initial $\delta^{18}O$ value of the water is derived from the average $\delta^{18}O$ composition of the respective aufeis since it represents the average $\delta^{18}O$ composition of the water feeding the individual aufeis. Also shown is the $\delta^{18}O$ composition of calcite precipitating in equilibrium with the evolving water during freezing. The $\delta^{18}O$ composition of calcite was calculated from the $\delta^{18}O$ of the water by correcting for the H_2O–$CaCO_3$ fractionation factor at 0 °C (34.4‰; Bottinga, 1968) and then converted to the VPDB-scale (Coplen et al., 1983). Dashed area indicates the measured $\delta^{18}O$ range in the cryogenic aufeis calcites.

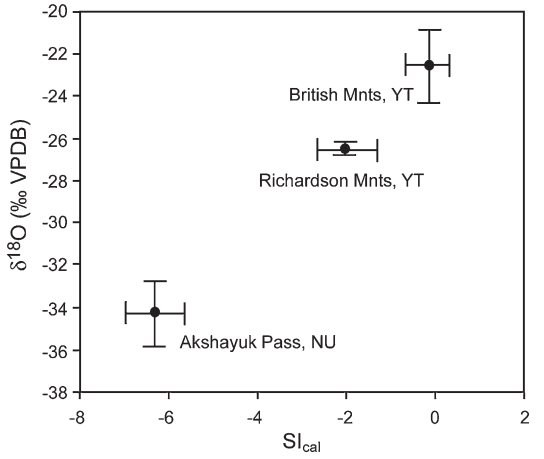

Fig. 10. Diagram showing the relation between the average $\delta^{18}O$ composition of the cryogenic aufeis calcites and the average calcite saturation index of the waters feeding the aufeis.

only takes place when freezing is a slow process. In addition to the $\delta^{18}O$ depletion trend, freezing imparts a concentration of solutes in the residual water, which consequently leads to an increase in the calcite saturation index. Therefore, it can be assumed that the $\delta^{18}O$ composition of calcite precipitating in equilibrium from a water that is highly undersaturated with respect to calcite, such as those from Little Fish Creek and Highway Glacier aufeis, will be depleted over the initial $\delta^{18}O$ composition of its parent water as calcite saturation will only be exceeded in the later stage of freezing.

To verify if the ^{18}O composition of cryogenic calcite is related to the initial calcite saturation state of their parent water, the geochemical partitioning that occurs during freezing was modeled using the PHREEQC computer code (Parkhurst and Appelo, 1999). Freezing was simulated by assuming no incorporation of solutes in the ice. During freezing, the solutes concentration and calcite saturation indices progressively increased as the solutes were partitioned in the residual water (Fig. 11). Extreme solutes enrichments (up to 60 times for Ca^{2+}) were found during the late stage of freezing, consistent with the freezing experiments of Hallet (1976) and Killawee et al. (1998). However, once calcite precipitation has occurred, the ionic composition of the solution will deviate from that shown in Fig. 11 as Ca^{2+} and HCO_3^- enrichments will cease. The effect of closed-system freezing on the $\delta^{18}O$ of the residual water was also numerically modeled, but the minor effect of CO_2 and calcite separation on the $\delta^{18}O$ of the residual was neglected. During freezing, the $\delta^{18}O$ composition is progressively depleted due to the Rayleigh fractionation on the residual water. Extreme depletion of up to 12‰ were found when the bulk of the water had frozen.

Based on the PHREEQC hydrogeochemical program, calcite supersaturation (SIcal > 0) is expected to occur in the early to mid-stage of freezing for waters that have an initial calcite saturation state close to 0, such as those located in carbonated environments (Fig. 11). This explains why the $\delta^{18}O$ composition of the cryogenic calcite collected from the British Mountains, such as the Babbage River and Fish Hole Creek aufeis, tends to reflect the initial $\delta^{18}O$ composition of their parent water (Fig. 9). But even in carbonated environments, the $\delta^{18}O$ composition of the cryogenic calcite might be slightly depleted with respect to the initial $\delta^{18}O$ composition of the parent water since calcite does not always precipitate

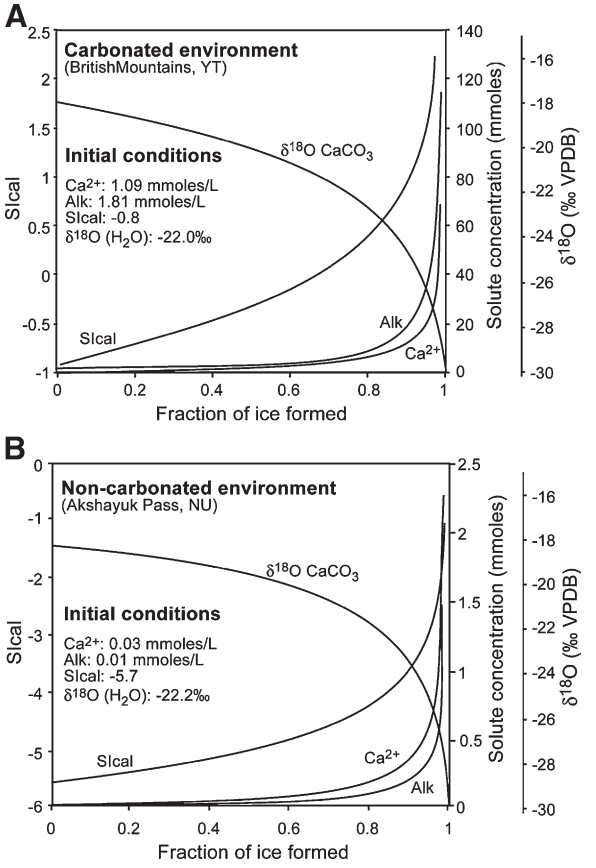

Fig. 11. The evolution of the SIcal and solute concentrations of water collected in the British Mountains (A) and Akshayuk Pass (B) during closed-system freezing as simulated by the PHREEQC hydrogeochemical software (Parkhurst and Appelo, 1999). The solubility product of calcite used by PHREEQC at 0 °C is $10^{-8.35}$. Also shown is the $\delta^{18}O$ composition of calcite precipitating in equilibrium from these solutions. The $\delta^{18}O$ composition of calcite is derived from the $\delta^{18}O$ of water during freezing under closed-system conditions according to the Rayleigh fractionation and was corrected for the H_2O–$CaCO_3$ fractionation factor at 0 °C (34.4‰; Bottinga, 1968) and then converted to the VPDB-scale (Coplen et al., 1983).

instantaneously when supersaturation is reached. Dreybodt et al. (1992) indicated that calcite precipitation tends to occur when the calcite saturation state of the water is in the 0.7 to 1.0 range, due to kinetic inhibition, such as the natural energy barrier preventing calcite nucleation (Berner, 1981) or high concentrations of dissolved impurities which might block potential crystal growth sites (Zuddas and Mucci, 1994). In non-carbonated environments (i.e. Akshayuk Pass), calcite supersaturation is reached only in the later stage of freezing, which is also when the $\delta^{18}O$ composition of the parent water becomes strongly depleted over its initial $\delta^{18}O$ composition (Fig. 11). Since calcite precipitation does not occur until the calcite saturation state exceeds 0, the $\delta^{18}O$ values of the cryogenic calcite in non-carbonated environments would be highly depleted with respect to the initial $\delta^{18}O$ composition of their parent water due to their low initial calcite saturation index. This was the case for the cryogenic aufeis calcite collected from the surface of Highway Glacier and Little Fish Creek aufeis (Fig. 9).

6.2. Carbon-13 fractionation during closed-system freezing

Previous studies on the $\delta^{13}C$ composition of cryogenic carbonates showed that open system freezing can imparts a severe ^{13}C enrichment in calcite over the bicarbonate-rich solution ($^{13}C_{DIC}$) as a result of either *i*) CO_2 degassing quickly during calcite precipitation which precludes ^{13}C equilibrium between the precipitating carbonate and the escaping CO_2 (Clark and Lauriol, 1992); *ii*) continuous escape of CO_2 during calcite precipitation in an open system (Rayleigh-type fractionation; Zak et al., 2004) or *iii*) repeated freeze–thaw events (Socki et al., 2001). However, under closed-system freezing, the ^{13}C fractionation between calcite and the escaping CO_2 is less severe. Zak et al. (2004) numerically modeled the effect of closed-system freezing on the $\delta^{13}C$ composition of cryogenic carbonates based on the assumption that all evolved CO_2 is kept within the system. The model showed that there was a progressive, but slight increase in the $\delta^{13}C$ composition (up to 4‰) of the cryogenic carbonates over the initial $\delta^{13}C_{DIC}$. Since the aggradation of aufeis occurs under a closed-system condition, the $\delta^{13}C$ of the precipitating cryogenic carbonates should tend to reflect that of the initial $\delta^{13}C_{DIC}$ of the parent water and the temperature at which calcite precipitated.

This was verified by calculating the initial $\delta^{13}C_{DIC}$ value of the parent water from which the cryogenic aufeis calcite precipitated using the following equation:

$$\delta^{13}C_{DIC} = \delta^{13}CCaCO_3 - 0.5\ (\varepsilon CO_2 - HCO_3^- + \varepsilon HCO_3^- - CaCO_3) \quad (4)$$

since carbon is evenly divided between two phases (calcite and CO_2) during calcite precipitation. Using the average $\delta^{13}C$ of the cryogenic aufeis calcite (-4.9 ± 2.1‰), this gives an initial $\delta^{13}C_{DIC}$ value in the -12.5‰ to -8.4‰ range for the parent water from which the cryogenic aufeis calcite precipitated. These initial $\delta^{13}C_{DIC}$ values are in the same range as the lower end-member of $\delta^{13}C_{DIC}$ measured in the waters feeding the aufeis (-10.6‰ to -0.1‰; Tables 1 and 2). This indicates that the precipitation of the cryogenic aufeis calcite occurred under closed-system freezing, which precludes an isotopic equilibrium with atmospheric CO_2 (i.e. a $\delta^{13}C_{DIC}$ enrichment of the parent water).

Radiocarbon measurements of cryogenic aufeis calcite collected from Highway Glacier aufeis further supports that they are formed under closed-system conditions. The cryogenic aufeis calcite deposits have ^{14}C activities in the 43.2 to 44.2 pMC range (TO-11968 and TO-11934), while the fracture-filling calcite has a ^{14}C activity of 4.4 pMC (TO-11933), which suggests that it is likely of a hydrothermal origin within the crystalline bedrock (Table 3). However, the ^{14}C activities of the cryogenic calcite deposits should have been near 100 pMC since their production is related to the formation of Highway Glacier aufeis. Aerial photographs and field observations indicate that

Table 3
Radiocarbon measurements of the cryogenic calcite collected from the surface of Highway Glacier aufeis and fracture-filling calcite

Location	Type	Latitude	Longitude	^{14}C activity (pMC)	Uncalibrated ^{14}C age	Laboratory number
Highway Glacier	Cryogenic aufeis calcite	66°41.81′N	64°58.67′W	44.2	6560±70	TO-11968
Highway Glacier	Cryogenic aufeis calcite	66°42.13′N	64°59.44′W	43.2	6750±330	TO-11934
Rundell Glacier	Fracture-filling calcite	66°40.34′N	65°01.12′W	4.4	25140±290	TO-11933

Note: The radiocarbon measurements were by accelerator mass spectrometry at IsoTrace Laboratory (University of Toronto). The ^{14}C activities are presented as pMC (percent Modern Carbon) and ^{14}C ages are presented as conventional ^{14}C ages in years BP using Libby's ^{14}C half-life of 5568 years.

Highway Glacier aufeis completely melts during the thaw season and rebuilds from subglacial meltwater circulating through a proglacial talik the subsequent winter. Therefore the groundwater that infiltrates in the subglacial environment would have a ^{14}C activity near 100 pMC and will dissolve the near ^{14}C-free fracture-filling calcite. Thus, a stoichiometric dissolution of the fracture-filling calcite with the subglacial meltwater will result in a dilution of the ^{14}C activity of the DIC of the subglacial parent water to values near 50 pMC. Given that the aggradation of aufeis occurs under closed-system conditions, the ^{14}C activity of the parent water will not re-equilibrate with modern atmospheric CO_2 as was it was observed for the $\delta^{13}C$ of the cryogenic calcites. Therefore, the ^{14}C activity of 43 to 44 pMC measured in the cryogenic calcite deposits suggests that the carbon is derived from a closed-system dissolution of the fracture-filling calcite, followed by closed-system precipitation.

7. Conclusion and implications in paleoclimatic studies

In this study the $\delta^{18}O$ and $\delta^{13}C$ composition of cryogenic aufeis calcite in relation to the initial $\delta^{18}O$, $\delta^{13}C_{DIC}$ and chemical composition of the waters feeding aufeis in a carbonated (western Canadian Arctic) and non-carbonated (southern Cumberland Peninsula) environment were examined. Under most circumstances, the $\delta^{18}O$ composition of cryogenic carbonates is estimated from the initial $\delta^{18}O$ composition of the parent water and temperature at which calcite precipitated. However, the $\delta^{18}O$ composition of cryogenic carbonates from a carbonated environment (Babbage River and Fish Hole Creek aufeis) shows a slight depletion over that of the $\delta^{18}O$ of the parent water, while cryogenic carbonates from a non-carbonated environment (Highway Glacier and Little Fish Creek aufeis) show a strong depletion in $\delta^{18}O$ values with respect to that of the initial $\delta^{18}O$ value of the parent water. This discrepancy between the $\delta^{18}O$ of the cryogenic carbonate and that of the parent is attributed to the nature of aufeis growth, the calcite saturation state of the parent water and kinetic inhibitions during carbonate precipitation. Given that the aggradation of aufeis occurs under closed-system freezing of perennial groundwater-fed springs upon exposure to cold air, the freezing of water imparts a progressive depletion in $\delta^{18}O$ in the residual water due to the removal of heavier isotopes into the ice and a concentration of solutes in the residual water, which leads to an increase in calcite saturation index. Therefore, carbonate that precipitate in equilibrium from water that has a low calcite saturation index will have a highly depleted $\delta^{18}O$ composition over that of the initial $\delta^{18}O$ values of the parent water. By contrast, the $\delta^{13}C$ composition of the cryogenic aufeis carbonates is not affected by solute partitioning during closed-system freezing, and tends to reflect that of the initial $\delta^{13}C_{DIC}$ value of the parent water.

These findings can possibly be extended to secondary carbonates in polar regions formed by intense evaporation, such as the calcareous crusts formed on the underside of clasts within the active layer (Bunting and Christensen, 1978). In such case, the $\delta^{18}O$ signature of the carbonate in non-carbonated environments would be enriched by several permil over that of the $\delta^{18}O$ composition of the parent water since evaporation is an highly fractionating process that leads to a progressive increase in $\delta^{18}O$ in the residual water.

In light of the evidence presented in this study, care must be taken when interpreting the $\delta^{18}O$ signature preserved in secondary carbonates in polar regions since the $\delta^{18}O$ composition of their parent water might have been modified by secondary processes (i.e. freezing or evaporation) prior to calcite being precipitated. As a result, the $\delta^{18}O$ composition of secondary carbonates cannot easily be used in conjunction with Dansgaard global $\delta^{18}O$–T °C relation to derive local mean annual air temperatures unless clear details about the chemical and isotopic composition of the parent waters are known. However, the $\delta^{13}C$ composition of secondary carbonates that precipitated under closed-system conditions can allow insights into the different water sources contributing to carbonate precipitation.

Acknowledgments

This work was funded by Natural Science and Engineering Research Council of Canada (NSERC) discovery grants to B. Lauriol and I.D. Clark, by an Ontario Graduate Scholarship (OGS) and Northern Scientific Training Program (NSTP) grant to D. Lacelle. We would like to thank W. Abdi, G. St-Jean, and P. Middlestead (G.G. Hatch Laboratory, University of Ottawa), B. Cousens (strontium analyses, Carleton University) and M. Alewany for their technical assistance. The radiocarbon measurements were made at IsoTrace (University of Toronto). J.F. Dion, J. Clark and C. Duchesne provided valuable field assistance. Special thanks to B. Etooangat and P. Smiley (Parks Canada) for providing logistical support during our stay in Auyuittuq National Park (research permit number ANP 2004-001). This manuscript benefited from the

constructive comments made by Dr. I. Fairchild and an anonymous reviewer. **[PD]**

References

Akerman, H.J., 1982. Studies on naledi (icing) in west Spitsbergen. Fourth Canadian Permafrost Conference Calgary, Canada. National Research Council of Canada, Ottawa, pp. 189–202.

Berner, R.A., 1981. Kinetics of weathering and diagenesis. In: Lasaga, A.C., Kirkpartick, R.J. (Eds.), Kinetics of Geochemical Processes. . Reviews in Mineralogy, vol. 8. Mineralogical Society of America, pp. 111–132.

Blake Jr., W., 2005. Holocene carbonate precipitates on Precambrian bedrock in the High Arctic: age and potential for paleoclimatic information. Geografiska Annaler 87A, 175–192.

Bottinga, Y., 1968. Calculation of fractionation factors for carbon and oxygen in the system calcite–carbon dioxide–water. Journal Physical Chemistry 72, 800–808.

Bunting, B.T., Christensen, L., 1978. Micromorphology of calcareous crusts from the Canadian High Arctic. Geologiska Foreningens Forhandlinger 100, 361–367.

Clark, I.D., Lauriol, B., 1992. Kinetic enrichment of stable isotopes in cryogenic calcites. Chemical Geology 102, 217–228.

Clark, I.D., Lauriol, B., 1997. Aufeis of the Firth River basin, northern Yukon, Canada: insights into permafrost hydrogeology and karst. Arctic and Alpine Research 29, 240–252.

Clark, I.D., Lauriol, B., Harwood, L., Marschner, M., 2001. Groundwater contributions to discharges in a permafrost setting, Big Fish River, N.W.T., Canada. Arctic, Antarctic, and Alpine Research 33, 62–69.

Clark, I.D., Lauriol, B., Marschner, M., Sabourin, N., Chauret, Y., Desrochers, A., 2004. Endostromatolites from permafrost karst, Yukon Canada: paleoclimatic proxies for the Holocene thermal hypsithermal. Canadian Journal of Earth Sciences 41, 387–399.

Coplen, T.B., Kendall, C., Hopple, J., 1983. Comparison of isotope reference samples. Nature 302, 236.

Courty, M.A., Marlin, C., Dever, L., Tremblay, P., Vachier, P., 1994. The properties, genesis and environmental significance of calcitic pendants from the High Arctic (Spitsbergen). Geoderma 61, 71–102.

Dansgaard, W., 1964. Stable isotopes in precipitation. Tellus 16, 436–468.

Dansgaard, W., 1982. A new Greenland deep ice core. Science 218, 1273–1277.

Dreybodt, W., Buhmann, D., Michaelis, J., Usdowski, E., 1992. Geochemically controlled calcite precipitation by CO_2 outgassing: field measurements of precipitation rates in comparison to theoretical predictions. Chemical Geology 97, 285–294.

Dyke, A.S., Andrews, J.T., Miller, G.H., 1982. Quaternary geology of Cumberland Peninsula, Baffin Island, District of Franklin. Geological Survey of Canada, Memoir 403 (32 pp.).

Environment Canada, 2004. Canadian Climate Normals 1971–2001. Canada Atmospheric Environment Service, Minister of Supply and Services Canada, Ottawa, Ontario, Canada.

Epica Community Members, 2004. Eight glacial cycles from an Antarctic ice core. Nature 429, 623–628.

Fairchild, I., Bradly, L., Spiro, B., 1993. Carbonate diagenesis in ice. Geology 21, 901–904.

Fisher, D.A., Koerner, R.M., Bourgeois, J.C., Zielinski, G., Wake, C., Hammer, C.U., Clausen, H.B., Gundestrup, N., Johnsen, S., Goto-Azuma, K., Hondoh, T., Blake, E., Gerasimoff, M., 1998. Penny Ice Cap cores, Baffin Island, Canada, and the Wisconsinan Foxe dome connection: two states of Hudson Bay ice cover. Science 279, 692–695.

Forman, S.L., Miller, G., 1984. Time-dependant soil morphologies and pedogenic processes on raised beaches, Broggerhalwoya, Spitsbergen, Svalbard archipelago. Arctic and Alpine Research 16, 381–393.

Hall, D.K., 1980. Mineral precipitation in North Slope river icings. Arctic 33, 343–348.

Hallet, B., 1976. Deposits formed by subglacial precipitation of $CaCO_3$. Geological Society of America Bulletin 87, 1003–1015.

Heldmann, J.L., Pollard, W.H., McKay, C.P., Andersen, D.T., Toon, O.B., 2005. Annual development cycle of an icing deposit and associated perennial spring activity on Axel Heiberg Island, Canadian High Arctic. Arctic, Antarctic, and Alpine Research 37, 127–135.

Hillaire-Marcel, C., Soucy, J.M., Cailleux, A., 1979. Analyse isotopique de concrétions sous-glaciaire de l'inlandsis laurentidiens et teneur en oxygène 18 de la glace. Canadian Journal of Earth Sciences 16, 1494–1498.

Hossein, R., Arn, K., Steinmann, P., Adatte, T., Follmi, K.B., 2004. Carbonate and silicate weathering in two presently glaciated, crystalline catchments in the Swiss Alps. Geochimica et Cosmochimica Acta 68, 1021–1033.

Jacobson, A.D., Blum, J.D., Chamberlain, C.P., Poage, M.A., Sloan, V.F., 2002. Ca/Sr and Sr isotope systematics of a Himalayan glacial chronosequence: carbonate versus silicate weathering rates as a function of landscape surface age. Geochimica et Cosmochimica Acta 66, 13–27.

Killawee, J.A., Fairchild, I.J., Tison, J.L., Janssens, L., Lorrain, R., 1998. Segregation of solutes and gases in experimental freezing of dilute solutions: implication for natural glacier systems. Geochimica et Cosmochimica Acta 62, 3637–3655.

Lauriol, B., Cinq-Mars, J., Clark, I.D., 1991. Les naleds du nord Yukon : Localisation, genèse et fonte. Permafrost and Periglacial Processes 2, 225–236.

Lauriol, B., Ford, D.C., Cinq-Mars, J., Morris, W.A., 1997. The chronology of speleothem deposition in northern Yukon and its relationships to permafrost. Canadian Journal of Earth Sciences 34, 902–911.

Marlin, C., Dever, L., Vachier, P., Courty, M.-A., 1993. Variations chimiques et isotopiques de l'eau du sol lors de la reprise en gel d'une chouche active sur pergélisol continu (Presqu'ile de Brogger, Svalbard). Canadian Journal of Earth Sciences 30, 806–813.

Nakai, N., Wada, H., Kiyosu, Y., d Takimoto, M., 1975. Stable isotope studies on the origin and geological history of water and salts in the Lake Vanda area, Antarctica. Geochemical Journal 9, 7–24.

Norris, D.K., 1975. Geology, Bell River, Yukon Territory and Northwest Territories. Map 1519A, scale 1 :250,000. Geological Survey of Canada, Energy Mines and Resources, Ottawa, Canada.

Norris, D.K., 1977. Geology, Blow River and Davidson Mountains, Yukon Territory, District of Mackenzie. Map 1516A, scale 1 :250,000. Geological Survey of Canada, Energy Mines and Resources, Ottawa, Canada.

Parkhurst, D.L., Appelo, C.A.J., 1999. User's guide to PHREEQC (Version 2): a computer program for speciation, batch-reaction, one-dimensional transport, and inverse geochemical calculations. U.S. Geological Survey Water-Resources Investigations Report 99-4259. 310 p.

Pollard, W.H., 1983. A study of seasonal frost mounds, North Fork Pass, northern interior Yukon Territory. Unpublished PhD Thesis, University of Ottawa.

Pollard, W.H., 2005. Icing processes associated with High Arctic perennial springs, Axel Heiberg Island, Nunavut, Canada. Permafrost and Periglacial Processes 16, 51–68.

Sharp, M., Tison, J.L., Fierens, G., 1990. Geochemistry of subglacial calcites: implications for the hydrology of the basal water film. Arctic and Alpine Research 22, 141–152.

Socki, R.A., Romanek, C.S., Gibson Jr., E.K., Golden, D.C., 2001. Terrestrial aufeis formation as Martian analog: clues from laboratory-produced C-13 enriched cryogenic carbonate. Lunar and Planetary Science XXXII abstract #2032. Lunar and Planetary Institute, Houston, TX.

Souchez, R.A., Lemmens, M., 1985. Subglacial carbonate deposition — an isotopic study of present-day case. Palaeogeography, Palaeoclimatology, Palaeoecology 51, 357–364.

Swett, K., 1974. Calcrete crusts in an arctic permafrost environment. American Journal of Sciences 274, 1059–1063.

St-Jean, G., 2003. Automated quantitative and isotopic (^{13}C) analysis of dissolved inorganic carbon and dissolved organic carbon in continuous flow using a total carbon organic carbon analyser. Rapid Communications in Mass Spectrometry 17, 419–428.

Tolsikhin, N.I., Tolsikhin, O.N., 1976. Groundwater and surface water in the permafrost region. Canada Inland Waters Directorate, Water Resources Branch, Ottawa. Technical Bulletin 97, 1–27.

Van Everdingen, R.O., 1974. Groundwater in permafrost regions of Canada. Permafrost Hydrology, Proceedings of a Workshop Seminar, Canadian National Committee, International Hydrological Decade. Environment Canada, Ottawa.

Van Everndingen, R.O., 1988. Perennial discharge of subpermafrost groundwater in tow small drainage basins, Yukon, Canada. Proceedings, 5th International Conference on Permafrost, August 1988, Trondheim, Norway, pp. 639–643.

Van Everdingen, R.O., Allen, H., 1983. Ground movements and dendrogeomorphology in a small icing area of the Alaska Highway, Yukon, Canada. Proceedings, 4th International Conference on Permafrost, July 1983, Fairbanks, USA, pp. 1292–1297.

Zak, K., Urban, J., Cilek, V., Hercman, H., 2004. Cryogenic cave calcite from several Central European caves: age, carbon and oxygen isotopes and a genetic model. Chemical Geology 206, 119–136.

Zuddas, P., Mucci, A., 1994. Kinetics of calcite precipitation from seawater: I. A classical chemical kinetics description for strong electrolyte solutions. Geochimica et Cosmochimica Acta 58, 4353–4362.